

Observation of optical chemical shift by precision nuclear spin optical rotation measurements and calculations

Junhui Shi,¹ Suvi Ikäläinen,² Juha Vaara,³ and Michael V. Romalis⁴

¹*Department of Chemistry, Princeton University, Princeton, NJ, USA*

²*Department of Chemistry, University of Helsinki, Finland*

³*Department of Physics, University of Oulu, Finland*

⁴*Department of Physics, Princeton University, Princeton, NJ USA**

Nuclear spin optical rotation (NSOR) is a recently developed technique for detection of nuclear magnetic resonance via rotation of light polarization, instead of the usual long-range magnetic fields. NSOR signals depend on hyperfine interactions with virtual optical excitations, giving new information about the nuclear chemical environment. We use a multi-pass optical cell to perform first precision measurements of NSOR signals for a range of organic liquids and find clear distinction between proton signals for different compounds, in agreement with our earlier predictions. Detailed first principles quantum-mechanical NSOR calculations are found to be in good agreement with the measurements.

PACS numbers: 31.15.ap, 33.57.+c, 76.70.Hb

The effect of light on nuclear magnetic resonance (NMR) has been the subject of considerable interest, as it can be used to further increase the power of NMR spectroscopy [1, 2]. While NMR frequency shifts due to laser light turned out to be too small to be easily measured [3], the inverse effect of optical rotation (OR) caused by nuclear spin polarization was observed in water and liquid ^{129}Xe [4]. The rotation of light polarization is similar to the Faraday effect caused by nuclear magnetization, but is enhanced by the hyperfine interaction between nuclear spins and virtual electronic excitations. Recent first-principles calculations of the nuclear spin OR (NSOR) predict different signals from chemically non-equivalent nuclei, opening the possibility of a new chemical analysis technique combining optical and NMR spectroscopy [5]. However, the signal-to-noise ratio (SNR) of NSOR detection has been poor in the first experiments utilizing low-field CW NMR [4] and in high-field pulsed experiments [6, 7]. NSOR differences between the same nuclei in different molecular positions have not been clearly observed [7].

Here we use a multi-pass optical cell [8, 9] to measure proton NSOR with an SNR greater than 15 after 1000 seconds of integration and perform systematic NSOR measurements on organic liquids with absolute uncertainty of 5%. Contrary to recent report [7], we find that the NSOR signals do not scale with the Verdet constant V of the liquid since the hyperfine interaction between electrons and nuclei is influenced by the chemical environment. The ratio of NSOR to Faraday rotation and to inductive ^1H signals ranges by more than a factor of 2 for the simple chemicals studied. We also apply the recent first-principles theoretical method [5] for calculation of NSOR and obtain results in good qualitative agreement with our measurements for both ^1H and ^{19}F spins.

Optical cavities have been used in the past to amplify optical dispersion effects [10, 11], but multi-pass cells

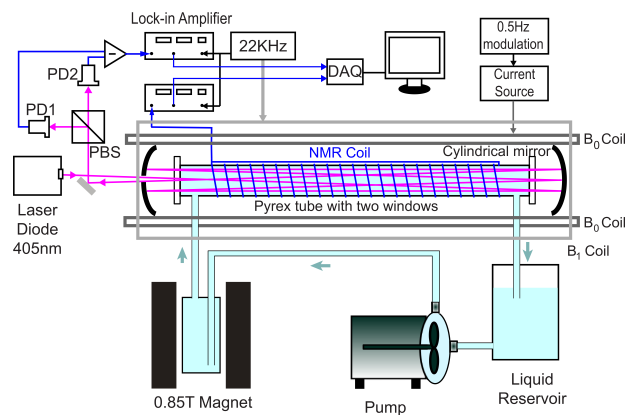


FIG. 1: Apparatus for measurement of NSOR in organic liquids. The multi-pass cell consists of two cylindrical mirrors with 40 cm separation and 50 cm radius of curvature, the sample tube is 22.5 cm long.

have a number of advantages [9]. They do not require locking the frequency of the laser to the optical cavity resonance or spatial mode matching of the laser beam to the cavity standing wave. They also do not require optimization of mirror reflectivity to achieve maximum power coupling into the cavity depending on losses. Our multi-pass cell consists of two cylindrical mirrors with a small hole in one of the mirrors to let the laser beam enter and exit the cell (see Fig. 1) [8]. The number of passes is determined solely by the distance between the mirrors, their curvature, and the twist angle between their axes of curvature. The laser wavelength is chosen to be 405 nm, since NSOR is enhanced at short wavelengths as $1/\lambda^2$. To reduce optical losses in our cell, the sample tube end windows have an anti-reflection coating on the outside surfaces. While optical absorption length in very pure liquids can exceed 100 meters at 405 nm [12], it is very sensitive to impurities. We adjusted the multi-

pass cell to have 14 passes for a total optical path length of 3.15 meters. The number of passes is determined by counting the number of beam spots on each mirror. In the measurements on water the initial laser intensity of 8 mW was reduced to 0.4 mW after the multi-pass cell; the transmission was similar for other chemicals studied. Note that the increase in the photon shot noise by a factor of 4.5 due to light absorption is still less than the 14-fold increase in the OR signal, demonstrating an increase of the SNR with the multi-pass cell. The NSOR detection method is based on a CW spin-lock technique, first developed in Ref. [4]. As shown in Fig. 1, the liquid is circulated continuously by a pump from a reservoir to a permanent pre-polarizing magnet, and then to a sample glass tube inside a uniform magnetic field $B_0 = 5$ G. An oscillating magnetic field is applied perpendicular to the B_0 field, so the nuclear spins are adiabatically transferred to the frame rotating at the NMR frequency as they enter the region of B_0 field. A solenoidal pick-up coil wound around the sample tube is used to measure the traditional NMR signal and determine the polarization for each flowing liquid [13].

The OR signal measured by a balanced polarimeter and the voltage across the pick-up coil are recorded by two lock-in amplifiers referenced to the NMR frequency. In addition, we modulate the B_0 field on and off resonance at 0.5 Hz to distinguish NMR signals from any backgrounds. For static liquids the OR noise is limited by photon shot noise, but it increases by about a factor of 2 during flow, likely due to small bubbles in the liquid. The signal-to-noise ratio for water is typically about 15 after one hour, while it is larger for other organic chemicals studied in this paper. The NSOR signals of ^1H in hexane and ^{19}F in perfluorohexane are shown in Fig. 2.

In addition to NSOR, we also measured regular Faraday OR in all liquids using the solenoid wound around the sample tube to create a known magnetic field. The measured V are used to calculate the minimum NSOR signal due to the classical dipolar field produced by nuclear

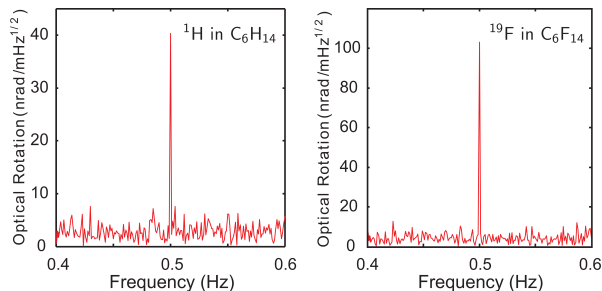


FIG. 2: Nuclear spin optical rotation signal of ^1H in C_6H_{14} and ^{19}F in C_6F_{14} after 1000 seconds of integration. Since B_0 field is modulated on and off the resonance at 0.5 Hz, the signal appears at this frequency. The SNR is about 16 and 24 for ^1H in C_6H_{14} and ^{19}F in C_6F_{14} respectively.

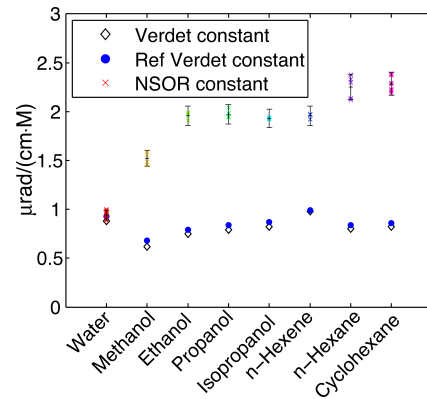


FIG. 3: ^1H NSOR constants (cross points and error bars), Faraday rotation Verdet constants (diamonds) from our measurements and reference Verdet constants (blue dots). All measurements of NSOR constants are shown for all chemicals to indicate the degree of experimental scatter.

spins, given by $\mathbf{B} = \mu_0\mathbf{M}$ for a long sample tube. Measurements of V in a single-pass geometry revealed that they are larger by 8.3% compared to multi-pass geometry, likely due to polarization impurity caused by multiple mirror reflections. We applied a +8.3% correction to all OR data in the multi-pass geometry. The NSOR were measured several times for each liquid, with periodic calibration by water NSOR measurements to check the long-term stability of the apparatus. In addition to the statistical error we assign a systematic error of 5% to each measurement that accounts for observed long-term changes in the signal amplitudes. We also find that our measured V are on average 5% smaller than literature values at 405 nm [14–16]. In Fig. 3 and [13] we summarize the measured NSOR amplitudes and V , as well as the Verdet constants from the literature. The NSOR data are scaled to 1 M concentration of fully polarized nuclei and V values are multiplied by the classical magnetic field produced by these nuclei in a long cylinder.

For water the Verdet constant of Faraday OR accounts for most of the NSOR signal, in agreement with [4], while in other chemicals NSOR is enhanced relative to Faraday OR due to hyperfine interactions. The data for water, methanol and ethanol are generally consistent with earlier first-principles theoretical calculations [5]. The enhancement of NSOR for hydrogens bound to carbon can be explained qualitatively by smaller electronegativity of C compared with O. This results in greater overlap of the electronic wavefunction with ^1H in CH_2 and CH_3 groups, giving a larger hyperfine interaction.

We also measure ^{19}F NSOR in perfluorohexane, which was first observed in [6] at high magnetic fields. The NSOR signal after 1000 s is shown in Fig. 2. The measured NSOR constant for ^{19}F is a factor of 6 larger than in hydrocarbons, while V is a factor of 3.5 smaller, consistent with earlier data for V in fluorocarbons [17]. The

enhancement of the NSOR signal by a factor of 57 relative to the OR due to the Faraday effect is partly due to stronger hyperfine interaction in heavier atoms [4] and partly due to high electronegativity of fluorine.

The OR angle Φ_{NSOR} of a beam of linearly polarized light arising due to nuclear spins can be calculated through the rotationally and ensemble-averaged antisymmetric polarizability [18–20]. The rotation per unit concentration n of the polarized nuclei N and per unit pass length l , $V_N = \Phi_{\text{NSOR}}/nl$, is given by [5],

$$V_N = -\frac{1}{2}\omega N_A c \langle I_{N,Z} \rangle \frac{e^3 \hbar \mu_0^2}{m_e 4\pi} \gamma_N \times \frac{1}{6} \sum_{\epsilon\tau\nu} \varepsilon_{\epsilon\tau\nu} \text{Im} \langle \langle r_\epsilon; r_\tau, \frac{\ell_{N,\nu}}{r_N^3} \rangle \rangle_{\omega,0}, \quad (1)$$

where ω is the frequency, $\langle I_{N,Z} \rangle$ is the average spin polarization, γ_N is the gyromagnetic ratio, and $\varepsilon_{\epsilon\tau\nu}$ is the Levi-Civita symbol. This expression is in terms of quadratic response theory [21], involving time-dependent electric dipole interaction with the light beam taken to second order, and the static hyperfine interaction

$$H_N^{\text{PSO}} = \frac{e\hbar \mu_0}{m_e 4\pi} \gamma_N \mathbf{I}_N \cdot \sum_i \frac{\ell_{iN}}{r_{iN}^3} \quad (2)$$

between the nuclear magnetic moment $\gamma_N \hbar \mathbf{I}_N$ and the electrons. For heavy-atom systems such as liquid Xe, relativistic formulation should be employed [22]. In the present systems the nonrelativistic form (1) is sufficient.

Eq. (1) does not include the long-range magnetization field discussed in Ref. [23]. In a long cylindrical sample this field equals $\mathbf{B} = \frac{1}{3} \mu_0 \mathbf{M}$, resulting in an additional Faraday rotation. Hence, a bulk correction V_B given by

$$V_B = \frac{\Phi_B}{nl} = \frac{1}{3} N_A \mu_0 \langle I_{N,Z} \rangle \hbar \gamma_N V, \quad (3)$$

should be added to V_N to be fully comparable to the experimental results.

Optimized geometries of the molecules were obtained with the Gaussian software [24] at the B3LYP/aug-cc-pVTZ level, while the Dalton program [25] was used for NSOR and V at 405 nm. In the latter, implementations of quadratic response functions were employed for the Hartree-Fock (HF), density-functional theory (DFT), and coupled-cluster (CC) methods from Refs. [26–28], respectively. DFT was used to obtain results of predictive quality for larger molecules. Therefore, its performance was assessed through more accurate but also more time-consuming *ab initio* CC singles and doubles (CCSD) calculations for water, methanol, ethanol, propanol and isopropanol. The DFT functionals BHandHLYP(50%), B3LYP (20%), and BLYP (0%) were used, where the percentages denote the amount of exact HF exchange admixture, which has been often seen to be the factor controlling DFT accuracy for hyperfine properties [5, 29].

Novel and compact sc. completeness-optimized (co) basis sets [30] were used to furnish near-basis-set limit results for V_N , which requires an accurate description of the electronic structure both at the nuclear sites and at the outskirts of the electron cloud. This is due to the involvement of both the magnetic hyperfine and electric dipole operators. The efficiency of co sets for magnetic properties has been verified in several studies [5, 22, 30–32]. The co-2 set (10s7p3d primitive functions for C–O; 10s7p3d for H) was developed in Ref. [31] for laser-induced ^{13}C shifts in hydrocarbons. The carbon exponents [31] are used here also for oxygen. Co-0 (C–O: 12s10p4d1f, H: 8s8p5d) was generated in Ref. [32] for basis-set-converged NSOR for first-row main-group systems, as calibrated by ^1H and ^{19}F NSOR calculations for the FH molecule.

To assess V_B , the Verdet constants were calculated at the BHandHLYP/co-2 and B3LYP/co-2 levels for all molecules, as well as at the CCSD/co-2 level for water, methanol, ethanol, propanol, and isopropanol [13]. V computed with the co-2 basis were combined with V_N obtained with co-0, as the former property is not as sensitive to the basis-set quality as NSOR.

Fig. 4 and Table 1 in [13] show the calculated NSOR. Weighted averages over all ^1H and ^{19}F nuclei of the molecules are reported. Furthermore, tables of V_N for the separate chemical groups are provided [13]. In most cases, the use of a basis set with higher quality leads to larger V_N . The only exception is water, where no systematic change is observed. Perfluorohexane shows a difference of ca. 10% between the two basis sets, while for the other molecules, the percentage ranges from 20–50%. In all cases other than perfluorohexane, the calculated true NSOR [Eq. (1)] is smaller than the experimental result. Adding the bulk correction V_B improves the agreement of BHandHLYP/co-0 and B3LYP/co-0 data with experiment (Figure 4), apart from the exaggerated B3LYP results for perfluorohexane and water. However, the use of BHandHLYP/co-0 for water results in a good agreement with the measurements, both due to the reduced true NSOR contribution as well as the more realistic V obtained at the BHandHLYP level (Table 12 in [13]). For the larger molecules, the experimental values are reproduced qualitatively. A detailed analysis would necessitate the incorporation of solvation and intramolecular dynamics effects via molecular dynamics simulations [32]. In the case of perfluorohexane, the known issues [29] of the present DFT functionals with the hyperfine properties of ^{19}F may contribute to the observed overestimation.

Tables 3–11 in [13] reveal that the largest NSOR occur in the CH_2 groups, while the hydroxyl groups display distinctly smaller values than either the methyl or methylene groups for all molecules. This supports the electronegativity argument for the relatively small V_{H} in water (*vide supra*). In perfluorohexane, however, the CF_3 -group feature a larger V_{F} than the CF_2 group. The different methylene groups in propanol and hexane, as

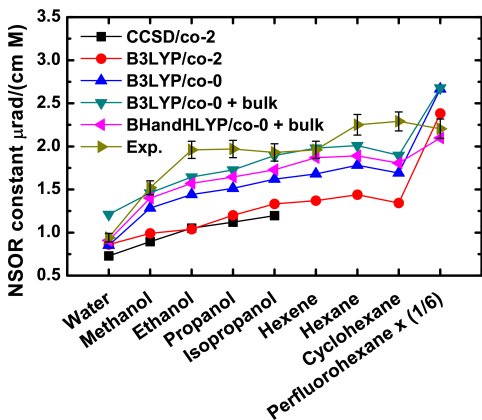


FIG. 4: V_N for all molecules at the B3LYP/co-2 and B3LYP/co-0 levels of theory, as well as V_N furnished with the bulk correction for B3LYP/co-0 and BHandHLYP/co-0. CCSD/co-2 data is given for the smaller molecules. Experimental values with error limits are also shown. Results for perfluorohexane are divided by a factor of six.

well as the axial and equatorial hydrogens in cyclohexane give similar results. Alteration in the magnitude of V_{1H} is observed for the CH_2 groups in hexene. The values for 1H in the methyl groups are rather similar for all the molecules, with isopropanol and hexane giving slightly larger NSOR than the other systems. The V_{1H} appropriate to the hydroxyl groups differ between the molecules, with ethanol and propanol giving very small signals. In hexene, the *cis*-type hydrogen shows a larger rotation than the other protons situated next to the double bond.

In summary, experimental NSOR signals do not scale with either the magnetic induction signal or the Verdet constant, but provide unique information about the nuclear chemical environment. A simple technique utilizing a multi-pass optical cell can be used to obtain signals with high SNR without a superconducting magnet. Shorter multi-pass cells with larger number of passes [9] can also be placed in superconducting magnets to obtain chemical shift information. Qualitative agreement with measured data is obtained with first-principles calculations using DFT calibrated against *ab initio* CCSD data. Hybrid DFT with 20% or 50% exact exchange is found to produce results closest to experiment. The bulk magnetization correction described in Ref. [23] is important. The 1HSOR is able to clearly distinguish hydroxyl group from methyl and methylene groups. Future application of these techniques to more complicated molecules can provide unique new information about their confirmation and electronic wavefunctions.

Support has been received from NSF grant CHE-0750191 (JS and MR), the graduate school in Computational Chemistry and Molecular Spectroscopy (SI), and Academy of Finland (JV). CSC (Espoo, Finland) provided the computational facilities.

- [1] W. Warren *et al.*, Science **255**, 1683 (1992).
- [2] A. Buckingham and L. C. Parlett, Science **264**, 1748 (1994).
- [3] W. Warren, D. Goswami, and S. Mayr, Mol. Phys. **93**, 371 (1998).
- [4] I. M. Savukov, S. K. Lee, and M. V. Romalis, Nature **442**, 1021 (2006).
- [5] S. Ikäläinen, M. V. Romalis, P. Lantto, and J. Vaara, Phys. Rev. Lett. **105**, 153001 (2010).
- [6] D. Pagliero, W. Dong, D. Sakellariou, and C. A. Meriles, J. Chem. Phys. **133**, 154505 (2010).
- [7] D. Pagliero and C. A. Meriles, Proc. Nat. Acad. Sci. (USA) **108**, 19510 (2011).
- [8] J. A. Silver, Appl. Optics **44**, 6545 (2005).
- [9] S. Li, P. Vachaspati, D. Sheng, N. Dural, and M. V. Romalis, Phys. Rev. A **84**, 061403 (2011).
- [10] E. Zavattini *et al.*, Phys. Rev. D **77**, 032006 (2008).
- [11] D. Pagliero, Y. Li, S. Fisher, and C. A. Meriles, Appl. Optics **50**, 648 (2011).
- [12] R. M. Pope and E. S. Fry, Appl. Optics **36**, 8710 (1997).
- [13] See supplementary material at [publisher inserts] for further experimental details, the experimental and computed data, and computational geometries.
- [14] E. Washburn, *International Critical Tables of Numerical Data, Physics, Chemistry and Technology(VI)*, National Research Council (1926).
- [15] E. G. Foehr and M. R. Fenske, Ind. Eng. Chem. **41**, 1956 (1949).
- [16] A. B. Villaverde and D. A. Donatti, J. Chem. Phys. **71**, 4021 (1979).
- [17] R. T. Lagemann, J. Am. Chem. Soc. **71**, 368 (1949).
- [18] A. D. Buckingham and P. J. Stephens, Annu. Rev. Phys. Chem. **17**, 399 (1966).
- [19] A. D. Buckingham, Phil. Trans. R. Soc. Lond. A **293**, 239 (1979).
- [20] T. Lu, M. He, D. Chen, T. He, and F.-c. Liu, Chem. Phys. Lett. **479**, 14 (2009).
- [21] J. Olsen and P. Jørgensen, J. Chem. Phys. **82**, 3235 (1985).
- [22] S. Ikäläinen, P. Lantto, and J. Vaara, J. Chem. Theory Comput. **91**, 8 (2012).
- [23] G.-h. Yao, M. He, D.-m. Chen, T.-j. He, and F.-c. Liu, Chem. Phys. **387**, 39 (2011).
- [24] M. J. Frisch, G. W. Trucks, and H. B. Schlegel *et al.*, *Gaussian 03*, Gaussian, Inc., Wallingford, CT (2004).
- [25] *DALTON2011, a molecular electronic structure program (2011)*, see <http://www.daltonprogram.org>.
- [26] H. Hettema, H. J. A. Jensen, P. Jørgensen, and J. Olsen, J. Chem. Phys. **97**, 1174 (1992).
- [27] P. Salek, O. Vahtras, T. Helgaker, and H. Ågren, J. Chem. Phys. **117**, 9630 (2002).
- [28] C. Hättig, O. Christiansen, H. Koch, and P. Jørgensen, Chem. Phys. Lett. **269**, 428 (1997).
- [29] J. Vaara, Phys. Chem. Phys. Chem. Phys. **9**, 5399 (2007).
- [30] P. Manninen and J. Vaara, J. Comput. Chem. **27**, 434 (2006).
- [31] S. Ikäläinen, P. Lantto, P. Manninen, and J. Vaara, J. Chem. Phys. **129**, 124102 (2008).
- [32] T. S. Pennanen, S. Ikäläinen, P. Lantto, and J. Vaara, submitted.

* Electronic address: romalis@princeton.edu